DEPOSITION OF SILICA FROM GEOTHERMAL WATERS ON HEAT TRANSFER SURFACES

by

J.S. GUDMUNDSSON

&

T.R. BOTT

Department of Chemical Engineering
University of Birmingham
Birmingham

Summary

Extended tests in specially designed equipment have been carried out on deposition from hot geothermal water from two different locations in Iceland, onto cooled heat exchanger surfaces. It is concluded that the deposition process is diffusion controlled followed by a dehydration reaction at the surface. The deposits consisted of a complex combination of elements with silica being the predominent compound. The solubility of amorphous silica may be influenced by the presence of cations. The nature of the surface of the scale appears to be related to the hydrodynamic conditions, a distinct "rippled" surface being obtained at one location.

Due to the increased turbulence generated by the rough scale surface an intial enhancement of heat transfer was obtained, but as deposition continued gradually increasing resistance to heat transfer was observed. Even over long periods (up to 2000 hours) no "equilibrium" value for the fouling resistance was obtained.

1. Introduction

As a result of the general energy situation throughout the world there is increased interest in the use of geothermal energy where it is available. Its application however, is not without its own problems.

In a recent review[1] on the utilisation of geothermal resources in Iceland, it was stated that low temperature waters (80-110°C), have traditionally been used for district heating purposes. Increasingly, however, geothermal areas producing high enthalpy steam/water mixtures are being explored and the steam used in industrial drying and electricity production. The utilisation and disposal of the residual water fraction has, presented some engineering difficulties.

The high temperatures (200-300°C) prevailing underground in areas producing steam/water mixtures, result in considerable amounts of solids being dissolved in the water, of which silica is the major constituent. When the water flows from a borehole to the surface partial flashing occurs and steam is formed, resulting in increased solids concentration and cooling of the geothermal water. The residual hot water becomes highly supersaturated with respect to silica, giving rise to rapid deposition on all surfaces[2]. The scale is hard and not easily removed by mechanical or chemical methods.

The significance of silica deposition is not limited to geothermal developments in Iceland. In the United States, Mexico, Japan, New Zealand and elsewhere, similar

geothermal resources are being exploited. The deposition problem is limited to geothermal areas producing steam/water mixtures and does not affect those areas producing predominantly steam. The former type represents probably most of the unexplored geothermal areas of the world. It has been suggested that silica deposition is the major constraint on the utilisation of geothermal energy[3].

2. Silica in Water

In any study of silica deposition it is necessary to have an appreciation of the physical chemistry and behaviour of silica in water. The principal form of dissolved silica in water is monosilicic acid H_4SiO_4 or $Si(OH)_4$, which is a weak acid and therefore practically undissociated in neutral solutions[4]. Geothermal waters are usually neutral or basic[5]. In basic solutions when pH > 9, silicic acid dissociates and increases the total solubility of silica considerably[6].

Solid silica can exist in a number of forms[7]. Quartz and amorphous silica are of interest in the present studies. In the high temperature areas producing steam/water mixtures the amount of silica dissolved in the geothermal water depends on the solubility of quartz[5]. However, amorphous silica is the form which precipitates from geothermal and other aqueous solutions on concentration and cooling[5, 7, 8, 9]. Silica deposition and fouling will occur in geothermal pipelines and production equipment when the concentration of silica exceeds the solubility of amorphous silica. The solubility of amorphous silica is much greater than that of quartz[10].

When a solution saturated with silica is cooled, the excess silicic acid will polymerize until a new equilibrium is reached[7, 10-13]. In acid solutions silica gel will be formed but in neutral and alkaline solutions the polymerization gives rise to negatively charged colloidal particles[11, 12], but excess silicic

acid will also deposit and form hard scales. The reaction involved is probably one of dehydration as is the polymerization process. In geothermal solutions supersaturated with silicic acid, there are therefore two competing removal processes; polymerization and deposition.

The role of colloidal silica in deposition is not clear. It has been suggested that colloidal silica does not form a hard scale and that the problem of silica scaling might be reduced by allowing supersaturated solutions to polymerize before passing through pipes and equipment where deposition occurs[14]. This can only reduce the problem since, generally the geothermal water is cooled further during utilisation.

The dissolution of silica in water may be expressed by the hydration reaction

$$SiO_2\ (s) + 2H_2O \rightleftharpoons H_4SiO_4 \qquad .....(1)$$

where solid silica is converted to monosilicic acid[11, 12, 15, 16, 17]. The solubility of amorphous silica (at temperatures in the range 25-305°C) can be expressed by the relation.

$$c \doteq 15.1 \times 10^3 \exp\left(\frac{-1354}{T}\right) \qquad .....(2)$$

where c is the concentration of silica (SiO_2) in mg/kg and T is temperature ^oK[10].

Geothermal fluids from high temperature areas producing steam/water mixtures have been classified as

low, intermediate and high solids waters[3]. The classification reflects changing composition from geothermal waters with compositions similar to ground water through concentrations similar to sea water and up to highly concentrated brines. It has been reported that the solubility of amorphous silica in sea water is about the same as in fresh water[7].

Geothermal waters contain most of the chemical consituents expected in fresh and sea water solutions. The solubility of amorphous silica in water can be lowered considerably by the addition of trace amounts of aluminium or iron and probably other trivalent cations[13, 17, 18, 19]. It seems probable that the formation of a very insoluable aluminium silicate on the surface of amorphous silica simply prevents the underlaying silica from passing into solution[11]. This aluminium silicate could be considered as a surface compound less soluable than amorphous silica[19]. Aluminium has been found to have much greater effect than iron in reducing the solubility of silica[18]. The amount by which the solubility of silica is reduced, depends on the pH value. The solubility is only reduced by an appreciable amount when the pH is in the range 4-10 with a minimum solubility at a pH value of about 9[13, 18].

3. Experimental Work

A plate heat exchanger and simulated tubular heat exchangers were used in the experimental investigations. Deposition and fouling studies were carried out at Svartsengi and Hveragerdi, both situated in the south-west of Iceland. These geothermal areas are within the active volcanic zone lying across Iceland and produce steam/water mixtures[1]. At Hveragerdi the geothermal fluid is of rain water origin but at Svartsengi the fluid originates from sea water.

The brine used at Svartsengi came from a 402 m borehole with a base temperature of 212°C. The steam/brine mixture was separated in a cyclonic separator with a small fraction of the brine used in the plate heat exchanger and tubular heat exchanger experiments. The exchangers were on the same site as the borehole and separator such that the brine, supersaturated with silica, passed through the exchangers seconds after being separated. The brine fed to the tube heat exchangers was obtained by flashing off the geothermal steam/brine mixture at 100°C, whereas the fluid entering the plate heat exchanger resulted from flashing at 150°C. Since both streams were from the same boreholes, the dissolved solids content of the brine fed to the tube heat exchanger was greater, as shown in Table 1.

At Hveragerdi the geothermal water was taken from the district heating mains[2]. The water comes from two boreholes about 500 m outside the town. These boreholes

are 400 and 695 m deep, both with a base temperature of about 200°C. The steam/water mixture from the boreholes is separated at atmospheric pressure, the water fraction being piped to the town and arriving in the experimental heat exchangers some 20-30 minutes later. Simulated tubular heat exchangers were used at Hveragerdi.

The tubular heat exchangers were manufactured from 316 stainless steel. The main tube of the exchangers was 12.7 mm O.D. tube 2 m long. The first 50 cm acted as an entry section and a further 150 cm was surrounded by a 19.1 mm O.D. cooling jacket. Both tubes had a 1.22 mm thick wall. The exchangers were covered with a 12.7 mm thick rock-wool insulating material. The tubes were mounted vertically and operated in a co-current mode at Svartsengi but in a counter-current mode at Hveragerdi. At the inlet and outlet of all streams, oil-filled thermometer pockets were located, extending into the centre of the flow steam. The thermometers were mercury-in-glass reading 0-100°C having 0.1°C divisions. From the heat exchanger tubes all streams were fed to a weighing tank and drain.

At Svartsengi the geothermal brine was fed directly from the cyclonic separator to the tubular heat exchangers. Similarly, the cooling water was fed directly from the water mains. At Hveragerdi, however, considerable fluctuations existed in the hot and cold water mains. Automatic pressure regulators were therefore installed at the hot and cold water inlets to the exchangers. With

the passage of time there was a tendency for the flow-rate of the geothermal waters, at both locations, to decrease gradually due to increased pressure drop resulting from deposition in the pipelines and exchangers. To overcome the problem flowrates were adjusted each day to the required value. The flowrate of the cooling waters remained constant during the experiments.

The plate heat exchanger used at Svartsengi was an Alfa-Laval P22 exchanger. The exchanger had 13 plates made of 316 stainless steel and 0.51 mm thick. The flow arrangement was such that the hot water entering the exchanger divided into two parallel streams crossing the exchanger three times while heating the cold water. The plate exchanger operated in counter-current mode. The cold water stream also divided into two parallel channels and crossed the exchanger three times.

Temperatures of all streams entering and leaving the exchanger were measured by mercury-in-glass thermometers immersed in oil filled pockets. From the plate heat exchanger both brine and cooling water were fed to a weighing tank and drain.

The heat exchanger tubes were used as received, as was the plate heat exchanger. The experimental method consisted of regular adjustment of the flowrates to the required values and measuring the inlet and outlet temperatures. Adjustments were made at least once every day, sometimes more often.

The composition of the geothermal waters used in the

experiments is given in Table 1 and the composition of the cooling waters is given in Table 2. The average experimental conditions measured in the deposition and fouling studies are given in Table 3.

Table 1 Composition of Geothermal waters used in the Experiments

Measurement	SVARTSENGI		HVERAGERDI
	Plate Heat Exchanger	Simulated Heat Exchanger Tubes	Simulated Heat Exchanger Tubes
pH/°C	7,65/20	7,50/25	9,46/23
SiO_2	569,5	581	305
Na	8100	9700	155,4
K^+	1630	1385	12,9
Ca^{++}	1182	1227,4	3,21
Mg^{++}	1,3	5,93	0,25
Cl^-	15920	16125	126,2
F^-	0,1	0,16	2,3
SO_4^{--}	33,3	37,6	54,9
CO_2^*	22,7	19,3	119,2
H_2S^{**}	0.1	0.1	4,74
Dissolved Solids	27856	29642	777,0

$*H_2CO_3 + HCO_3^- + CO_3^{--}$

$**H_2S + HS^- + S^{--}$

All concentrations in mg/kg

Table 2 Composition of Cooling Waters used in the Experiments

	SVARTSENGI	HVERAGERDI
pH/°C	7,63/20	7,21/18
SiO_2	34,5	27
Na^+	133,3	12,9
K^+	6,5	1,2
Ca^{++}	22,6	9,8
Mg^{++}	22,6	0,33
Cl^-	233,0	13,4
F^-	0,14	0,30
SO_4^{--}	35,6	5,7
CO_2^*	53,7	36,1
H_2S^{**}	-	0,1
Dissolved Solids	574,5	100

$*H_2CO_3 + HCO_3^- + CO_3^{--}$

$**H_2S + HS^- + S^{--}$

All concentrations in mg/kg

Table 3 Experimental parameters

Experiment	T_i (°C)		T_o (°C)		W(kg/s)		t(h)
	In	Out	In	Out	Hot	Cold	
Svartsengi 2	90.3	72.6	18.0	31.5	0.1330	0.1763	791
" 3	90.9	69.0	20.1	30.5	0.1089	0.1852	766
" 4	152.1	44.0	16.4	95.4	0.4420	0.5827	1080
Hveragerdi 1	80.6	67.9	12.4	24.7	0.1343	0.1473	2035
" 2	79.8	62.0	12.6	22.4	0.0730	0.1476	2035
" 3	79.0	44.1	12.6	19.2	0.0266	0.1486	2035

4. Basis of Calculations

The physical properties of sea water solutions have been determined by several authors in terms of salinity (dissolved solids) and are presented in the form of empirical equations[20-24]. These equations have been used to determine the physical properties of the solutions used in the present work.

The overall heat transfer coefficient of a heat exchanger is usually calculated from an equation of the form

$$\frac{1}{U_i} = \frac{1}{h_i} + \frac{A_i}{h_w A_w} + \frac{A_i}{h_o A_o} + R_f \quad .....(3)$$

where

h is the film heat transfer coefficient

U is the overall heat transfer coefficient

A is the area

R_f is the fouling resistance due to deposits and the enhancement due to surface roughness[25].

Subscripts i, o and w refer to inside, outside and wall respectively.

The individual heat transfer coefficients in circular tubes can be evaluated from the expression.

$$Nu = 0.0225\ Re^{0.795}\ Pr^{y} \quad .....(4)$$

and $$y = 0.495 - 0.0225 \ln Pr \quad .....$$

which correlate an extensive set of data by about ± 10 percent[26, 27].

The above expression was tested against experimental

data obtained on tube heat exchanger number 1 at Svartsengi. The clean heat exchanger was tested by varying the brine flowrate, while the cooling water flowrate was at maximum, and measuring inlet/outlet temperatures and flowrates of all streams. This gave the overall heat transfer coefficient at different brine flowrates. The same procedure was carried out at various cooling water flowrates and maximum brine flowrate. The ratio of the experimental and predicted overall heat transfer coefficients is plotted in Figure 1. For Reynolds numbers greater than 1×10^4 the experimental coefficient was about 10 percent higher than the predicted coefficient from equation 4. This was probably due to the natural roughness of the heat exchanger tube. The heat balance ratio hot/cold of the rate of heat transfer Q was 0.930 on average.

The individual heat transfer coefficients for plate heat exchangers can be obtained from correlations similar to the expression given above, except that the constants will be different. Because of the great difference existing in the individual design of plate heat exchangers there are several correlations available for the different types of exchangers. The following correlation can be used, for the prediction of heat transfer coefficients in typical plate heat exchangers(28)

$$Nu = 0.28\ Re^{0.65}\ Pr^{0.4} \qquad .....(5)$$

The characteristic dimension in the above correlation is usually taken as twice the distance between adjacent plates

in the exchanger. To estimate the velocity component in the Reynolds number the available flow area is taken as the projected width of the plate, times the distance between adjacent plates.

The experimental data obtained at Svartsengi and Hveragerdi consisted essentially of flowrate and temperature measurements. A computer program was written to process the data. All physical properties were determined at average bulk temperatures and all Reynolds numbers were based on the clean tube diameter. The heat exchanged between the geothermal and cooling waters was calculated and used to evaluate the experimental overall heat transfer coefficient

$$U_e = \frac{Q}{A \Delta T} \qquad .....(6)$$

where Q(kW) is the rate of heat transfer and $T(^{o}C)$ the log. mean temperature driving force. The subscript i is omitted for convenience.

The individual heat transfer coefficients h_i and h_o in equation 3 were calculated from equations 4 and 5 for the tube and plate heat exchangers, respectively. The wall heat transfer coefficients h_w were calculated from the wall thickness and thermal conductivity. From these individual coefficients the clean overall heat transfer coefficient U_c was determined from equation 3, where R_f was taken as zero. Equation 3 was rearranged and written as

$$R_f = \frac{1}{U_e} - \frac{1}{U_c} \qquad .....(7)$$

and the fouling resistance calculated. No correction was made for natural roughness in evaluating U_c since the fouling resistance includes the competing effects of deposition and enhancement. No allowance was made for any fouling on the cooling water side as no fouling was observed; the changes are attributed to the geothermal water fouling.

The average of the calculated heat transfer parameters are given in table 4. These values indicate the sort of conditions at which the fouling data were obtained. The following physical dimensions were used in calculations involving the tubular exchangers; inside tube diameter 1.0262 cm, heat transfer area 483.59 cm^2, outside tube effective diameter 0.7824 cm. The thermal conductivity of the stainless steel was taken as 0.0159 (kW/m ^oC). With the wall thickness of 1.22 mm the wall resistance was R_w = 0.0767 $(kW/m^{2o}C)^{-1}$. The following dimensions were used in the plate exchanger calculations; effective diameter 5.88 mm and total heat transfer area 1.0813 m^2. The wall heat transfer resistance was R_w = 0.0321 $(kW/m^{2o}C)$.

Using the calculated values of the various film coefficients and the resistance of the metal wall it is possible to estimate the wall temperature; these are given in Table 4. The estimated wall temperatures can be seen to be very much lower than the saturation temperature of the geothermal water.

Table 4 Calculated parameters

Experiment	Q(kW)		$\frac{Q_{hot}}{Q_{cold}}$	U_e (kW/m^2°C)	Re		h(kW/m^2°C)		T_s (°C)	T_w (°C)
	Hot	Cold			Hot	Cold	Hot	Cold		
Svartsengi 2	9,202	9,886	0,931	3.22	44293	17104	10.59	9.258	143	32
" 3	9,105	9,271	0,982	3.14	39036	17849	8.982	9.608	143	26
" 4	194,0	193,2	1.004	5.31	6673	5456	12.55	13.16	140	35
Hveragerdi 1	7,050	7,469	0.944	2.98	43650	12335	10.77	7,535	74	36
" 2	5.609	6.001	0.935	2.51	22605	12021	6.496	7.454	74	24
" 3	3.772	4.091	0.922	1.62	7299	11628	2.758	7.369	74	-

5. Results

The results from the tube heat exchangers at Svartsengi, Runs 2 and 3, are plotted on Figure 2. The fouling resistance R_f calculated from equation 7 is plotted with time. At time zero the fouling resistance in both runs was negative but then increased steadily and assumed a positive value at 500 and 700 hours at Reynolds numbers 44,293 and 39,036, respectively. If the initial fouling resistance is taken as zero, the results suggest a fouling resistance of approximately 0.08 $(kW/m^{2o}C)^{-1}$, for both runs, after about 800 hours. It would therefore appear that changing the Reynolds number over the relatively small range of Runs 2 and 3, does not have much effect.

The calculated fouling resistance for the plate heat exchanger, Run 4, is also plotted in Figure 2. At time zero the fouling resistance has a finite value indicating that the correlation used in the fouling resistance calculations, equation 5, overpredicts the exchanger performance. The fouling resistance increases steadily in an apparent linear fashion. If the initial fouling resistance is taken as zero, the results suggest a fouling resistance of 0.08 $(kW/m^{2o}C)^{-1}$ after about 1000 hours.

The results on the heat exchanger tubes at Hveragerdi are quite different from those at Svartsengi. The fouling resistance for Runs 1-3 are plotted with time in Figures 3-5. The average Reynolds numbers of these runs were 43,650, 22,605 and 7299 respectively. To show a typical

set of data from which the fouling resistance plots were obtained, the heat transfer coefficients and flowrates, expressed by Reynolds number, for Run 2 at Hveragerdi, are plotted in Figure 6.

The fouling resistance plots for Runs 1 and 2 at Hveragerdi are "spoon" shaped and not similar to any fouling curves reported in the literature. After a short initiation period of 50 and 100 hours, respectively, both plots show enhanced heat transfer with maximum enhancement occuring at 200-400 hours. After the enhancement period there is a steady rise in fouling resistance in both experiments with little evidence of an asymptotic value having been reached even after 2000 hours of continuous operation. By assuming that the initial fouling resistance for Runs 1 and 2 was zero, the values obtained after 2000 hours would be 0.42 and 0.68 $(kW/m^{2o}C)^{-1}$ respectively.

The plot for Run 3 at Hveragerdi shown in Figure 5 was obtained under similar conditions as Runs 4 and 2, except that the Reynolds number was very much lower at 7299. Again, there is an apparent linear initiation period lasting for about 800 hours, with enhanced heat transfer lasting for a similar period. It would appear that after about 2000 hours the enhancement has disappeared and the heat transfer conditions returned to those at the start of the experiment.

6. Examination of Deposits

Deposits collected from the experimental heat exchangers at Svartsengi and Hveragerdi were examined microscopically and analysed for the main chemical constituents. X-ray diffraction work showed deposits from both locations to be completely amorphous. Gravimetric analysis of deposits, heated at 110°C for 1 hour, showed the silica contents at Svartsengi and Hveragerdi to be 86.9 and 59.4 percent, respectively.

Scanning electron micrographs of deposits from plate and tube exchangers at both locations, are shown in Figures 7-9. The three deposits show distinct topographical differences. The tube deposit from Run 2 at Svartsengi is globular in appearance and probably non-porous. Optical micrographs, of a polished cross-section of the plate exchanger deposit suggested a porous structure.

The tube exchanger deposit from Run 1 at Hveragerdi in Figure 9 shows a structure quite different from those at Svartsengi. The surface of the deposit consists of narrow ridges rising above a relatively uniform but rough area. A better view of the deposit is shown in Figure 10 (a photograph of 12.7mm O.D. in exchanger tube longitudinally cut). The direction of flow is from left to right. It is seen that the ridges or ripples are aligned transversely to the direction of flow and are apparently evenly spaced in the flow direction. To study this rippled deposit further, a polished cross-section from the pipe was examined in an optical microscope. The average spacing and height of the ripples were found to be

0.87mm and 0.123mm respectively. In cross-section the ripples were not symmetrical but leaned slightly against the direction of flow.

The deposit thickness in all experiments increased from inlet to outlet. This was most apparent in the plate exchanger at Svartsengi and the tube exchangers at Hveragerdi. The deposits examined were taken from downstream locations. The maximum thickness of the plate exchanger deposit was 0.4-0.5mm. The uniform area of the rippled deposit examined showed the maximum thickness to be 0.25-0.3mm.

Microprobe (X-ray spectra) was employed to examine qualitatively all the deposits for elemental composition. Deposits from both locations were very rich in silicon with small amounts of aluminium, calcium, potassium and sodium. The X-ray spectra showed that the concentrations of elements other than silicon was greater in the Hveragerdi deposits which also included some iron and titanium.

7. Discussion

The saturation temperature T_s of the geothermal water at Hveragerdi has been calculated from equation 2 and is given in Table 4. A comparison with the average inlet bulk temperature, as given in Table 3, shows the water to be undersaturated by about 5°C when entering the tubular exchangers.

No deposition should therefore occur in the hot water mains feeding the exchangers. With pH > 9 some of the silicic acid in solution should be dissociated and therefore increase the solubility. However, experience at Hveragerdi has shown that considerable deposition occurs in the hot water mains[2]. The solubility of silica at Hveragerdi is therefore lower than that given by equation 2.

The presence of small amounts of aluminium may lower the solubility of silica, as suggested earlier. Analysis for aluminium in the water is not available but the X-ray spectra reported in section 6 showed that aluminium was present. The pH of the water at Hveragerdi was in the range where the solubility is most affected by the presence of trivalent cations. It is therefore clear that the solubility of amorphous silica in geothermal water is not necessarily represented by equation 2, although it was derived from an extensive set of data. At Svartsengi no observations were made to confirm the applicability of equation 2.

It is important to appreciate the form of the depositing silica, molecular or colloidal, when discussing a possible deposition mechanism. Experience in Iceland of geothermal waters supersaturated with molecular silica, at conditions similar to those at Svartsengi and Hveragerdi, has shown that the excess silicic acid polymerizes to colloidal forms in almost one hour. At Svartsengi the experimental conditions were such that the geothermal brine passed through the exchangers immediately after separation at the well-head. All the silica depositing must therefore have been present in molecular form as silicic acid. At Hveragerdi some colloidal silica might have been present since deposition occurred in the pipeline feeding the exchangers and up to 30 minutes had passed since the water was separated at the well-head. But the bulk of the silica depositing must have been molecular since super-saturation occurred in the exchangers.

The fouling resistance for the plate and tube heat exchangers at Svartsengi in figure 2 increases linearly with time to reach similar values of ~ 0.08 $(kW/m^2\ ^oC)^{-1}$ in 1000 and 800 hours, respectively. This appears to suggest control by the same deposition mechanism. It was observed that the plate exchanger deposits were thicker than those in the tube exchangers. But as already noted, the plate exchanger deposits were also more porous. It was not possible to assess whether or not the same amount of deposition had occurred in the two types of exchangers. The tubular exchangers at Svartsengi were operated at average Reynolds number 44293 and 39036. These Reynolds number values were probably too close for a comparison to be made with respect

to the deposition mechanism in terms of Reynolds number.

At Hveragerdi runs 1 and 2 were obtained at Reynolds number 43650 and 22605, respectively. Figures 3 and 4 show that the lower Reynolds number run produces a more distinct "spoon" shaped curve. These results emphasize the dual nature of the fouling resistance; the competing factors of reduced heat transmission due to an insulating layer of deposit and the enhanced heat transfer due to increased surface roughness. It could be argued that because of the rippled deposit structure at Hveragerdi the inside heat transfer coefficient was enhanced to a greater extent at the higher Reynolds number value such that the apparent fouling resistance became less. While the data supports this argument at positive fouling resistance values the opposite appears to be true at negative values. Run 3 at Hveragerdi was conducted at Reynolds number 7299 and resulted in a much lower fouling resistance than runs 1 and 2. This may indicate that at these conditions mass transfer controls the deposition process. However, the data are much too complex and few in number for any conclusions about the deposition mechanism to be made.

An important consideration in deposition and fouling studies must be the increased fluid velocity at constant mass flow conditions when the available flow area decreases due to deposition. In run 1 at Hveragerdi the maximum deposit thickness was $\sim$ 0.3mm while the clean tube diameter was 10.262mm. The inside heat transfer coefficient increased therefore by $<$ 5 percent during the 2035 hours of the run. The implications for the plate exchanger at Svartengi were different. The effective plate spacing diameter was 5.88mm

while the maximum deposit thickness after the 1080 hours experimental period was ∿ 0.5mm. The reduced flow area could have increased the heat transfer coefficient by as much as 27 percent. Clearly, the effect of diameter reduction may be ignored in the tubular experiments but the reduced flow area has an important influence in the latter part of the plate exchanger experiments.

It has been shown that the silica depositing in the present experiments was in the form of molecular silicic acid. The solubility of silica in water increases with temperature. Deposition occurs, therefore, as a result of silica supersaturation when the geothermal water is cooled. Deposition was found to be heavier at the downstream end of the exchangers where the supersaturation was greatest. Where the deposit structure was non-rippled, deposition increased linearly with time. This implies that deposition release from the surface was negligible. It is suggested that silica deposition consists of diffusion of molecular species to the surface where a dehydration reaction occurs. The fouling resistance measured at Hveragerdi must be treated as a special case because of the rippled structure, although the basic mass transfer and reaction mechanism must also hold.

It is well known that pipes with repeated rib roughness elements give greater transfer rates in turbulent flow than pipes with the same height sand grain roughness[29-31]. The transfer rates are found to be greatest when the ratio of spacing to height of the roughness corresponds to the distance at which reattachment occurs downstream from a

roughness element[31]. (Reattachment occurs at 6-8 roughness heights downstream from an element[30]). The ratio of ripple spacing to height for the deposit in Run 1 at Hveragerdi was 7.1. It has been found that reattachment might occur at the ratio of 7.2[32] or 7.5[33] suggesting that the ripples are formed due to the phenomena of flow separation and reattachment.

The pressure drop in pipes with rippled surfaces is much greater than in pipes with the same height sand grain roughness[34]. Comparison of friction factor correlations[30] shows that when the friction factor is independent of Reynolds number, rippled surfaces may give 50 percent greater pressure drops. The rippled silica deposits from Run 1 at Hveragerdi gave a 170 percent higher pressure drop in the fully turbulent region that was calculated for sand grain roughness[34] with the same roughness of 0.123mm[31].

8. Conclusions

The following main conclusions may be derived from the experimental work:

1. The nature of the deposit depends on the hydrodynamic conditions and the degree of supersaturation e.g.
   (a) The fouling resistance at Svartsengi increased linearly with time. The deposits were globular and rough.
   (b) Rippled deposits were formed at Hveragerdi where the fouling resistance with time curve was spoon-like in shape.
2. The solubility of amorphous silica in geothermal waters may be lowered by the presence of cations, particularly aluminium and iron.
3. The process of silica deposition on a surface may involve diffusion from the bulk solution followed by a dehydration reaction at the surface.

References

(1) J.S. Gudmundsson, Applied Energy, 2 (2) (1976) 127.

(2) S. Thorhallsson, K. Ragnars, S. Arnorsson H. Kristmannsdottir Second U.N. Symp. Development Use Geothermal Resources, San Fransisco, (May 20-29 1975).

(3) J.S. Gudmundsson, T.R. Bott, I.Chem.E. Symp.Ser. No. 48 (1977).

(4) S.A. Greenberg, J. Phys. Chem. 61(1957) 196.

(5) S. Arnorsson, U.N. Symp. Development Utilisation Geothermal Resources, 2 (1) Pisa (1970).

(6) G.B. Alexander, W.H. Heston, R.K. Iler, J. Phys. Chem., 58 (1954) 453.

(7) K.B. Krauskopf, Geochimica et Cosmochimica Acta, 10 (1-2) (1956) 1.

(8) D.E. White, W.W. Brannock, K.J. Murata, Geochimica et Cosmochimica Acta, 10 (1-2) (1956) 27.

(9) R.O. Fournier, J.J. Rowe, Am. J. Sci. 264(1966) 685.

(10) A.G. Volosov, I.L. Khodakovshiy, B.N. Ryzhenko, Geochemistry International, 9 (1972) 362.

(11) R.K. Iler, "The Colloid Chemistry of Silica and the Silicates", Cornell University Press, Ithaca,N.Y.(1955).

(12) R.K. Iler, "Colloidal Silica", Surface and Colloid Science, 6 Editor E. Matijevic, Wiley (1973).

(13) G. Okomoto, T. Okura, K. Goto, Geochimica et Cosmochimica Acta 12 (1957) 123.

(14) T. Yangase, Y. Suginohora, K. Yangase, U.N. Symp. Development Utilisation Geothermal Resources, Piza(1970).

(15) S. Kitahara, Rev. Phys. Chem. Japan 30 (1960) 131.

(16) G.W. Morey, R.O. Fournier, J.J. Rowe, Geochimica et Cosmochimica Acta, 26 (1962) 1029.

(17) C.M. Jephcott, J.H. Johnston, Arch. Ind. Hyg. Occupational Med., 1 (1950) 323.

(18) L.H.P. Jones, K.A. Handreck, Nature, 198 (1963) 852.

(19) R.K. Iler, J. Colloid Interface Sci., 43 (1973) 399.

(20) L. Grunberg, 3rd. Int. Symp. Fresh Water Sea, 1 31 Dubrovnik (Sept. 1970).

(21) D.T. Jamieson, J.S. Tudhope, R. Morris, G. Cartwright, Desalination, 7 (1969/70) 23.

(22) D.T. Jamieson, J.S. Tudhope, Desalination, 8(1970) 393.

(23) J.D. Isdale, C.M. Spence, J.S. Tudhope, Desalination, 10 (1972) 319.

(24) J.D. Isdale, R. Morris,Desalination, 10 (1972) 329.

(25) R.A. Walker, T.R. Bott, Chem. Engr. No. 271 (1973) 151.

(26) M. Everett, Chem. Engr. No. 159, (1969). 159.

(27) Engineering Sciences Data Unit, "Forced Convection Heat Transfer in Circular Tubes", Part 1: Correlations for Fully-Developed Turbulent Flow - Their Scope and Limitations", Item No.67016 (1967).

(28) A. Cooper, Chem. Engr. No. 285 (1974) 280.

(29) J.T. Davies, "Turbulence Phenomena", Academic Press,(1972).

(30) R.L. Webb, E.R.G. Eckert, R.J. Goldstein, Int. J. Heat Mass Trans. 14 (1971) 601.

(31) J.S. Gudmundsson, I.H. Newson, T.R. Bott, UKAEA Report AERE-R 8703, (March 1977).

(32) D. Wilkie, Proc. 3rd Int. Heat Transfer Conf. Chicago, (Aug. 1966).

(33) M.J. Lewis, J. Heat Transfer, 97 (1975) 249.

(34) H. Schlicting, "Boundary-Layer Theory", McGraw-Hill, 6th edition, (1968).

Nomenclature

A	Area for heat transfer
h	Film heat transfer coefficient
$\bar{h}$	Mean film heat transfer coefficient
Nu	Nusselt number
Pr	Prandtl number
Q	Rate of heat transfer
$\bar{Q}$	Average rate of heat transfer
R_f	Fouling resistance
Re	Reynolds number
$\bar{Re}$	Mean Reynolds number
t	Time
T	Absolute temperature
T	Average absolute temperature
ΔT	Temperature difference
U	Overall heat transfer coefficient
$\bar{U}$	Mean overall heat transfer coefficient
W	Mass flow rate
y	Exponent

Subscripts

e	Experimental
c	Clean
i	Inside
o	Outside
s	Saturation
w	wall

Acknowledgements

The authors would like to express their thanks to the National Energy Authority (Orkustofnun) in Iceland for providing experimental facilities, to the Science Research Council and the Heat Transfer and Fluid Flow Service, Harwell for the provision of funds to enable the work to be carried out.

Figure Captions

Figure 1 Ratio of experimental: predicted heat transfer coefficient vs Reynolds number.

Figure 2 Fouling resistance vs time at Svartsengi.

Figure 3 Fouling resistance vs time at Hveragerdi - Run 1.

Figure 4 Fouling resistance vs time at Hveragerdi - Run 2.

Figure 5 Fouling resistance vs time at Hveragerdi - Run 3.

Figure 6 Overall heat transfer coefficients and Reynolds numbers vs time at Hveragerdi - Run 2.

Figure 7 Tube exchanger deposit from Run 2 at Svartsengi x 280.

Figure 8 Plate exchanger deposit x 280.

Figure 9 Tube exchanger deposit from Run 1 at Hveragerdi x 280.

Figure 10 Section of tube with deposit from Run 1 at Hveragerdi.

Note on Figures

All but two (number 1 and 6) of the Figures in this paper are presented elsewhere in the Thesis. To save space these are not repeated here, but instead the appropriate Thesis Figure numbers given in the following table:

Paper	Thesis
Fig 1	Included
Fig 2	Part III Fig 1
Fig 3	Part III Fig 2
Fig 4	Part III Fig 3
Fig 5	Part III Fig 4
Fig 6	Included
Fig 7	Part III Fig 5a
Fig 8	Part III Fig 5b
Fig 9	Part III Fig 5c
Fig 10	Part IV Fig 3

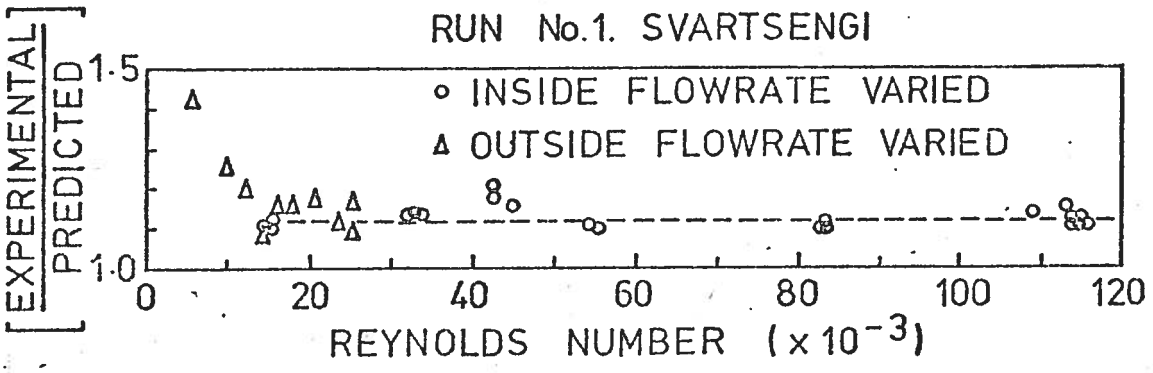

FIG. 1. RATIO OF EXPERIMENTAL / PREDICTED HEAT TRANSFER COEFFICIENT vs REYNOLDS NUMBER.

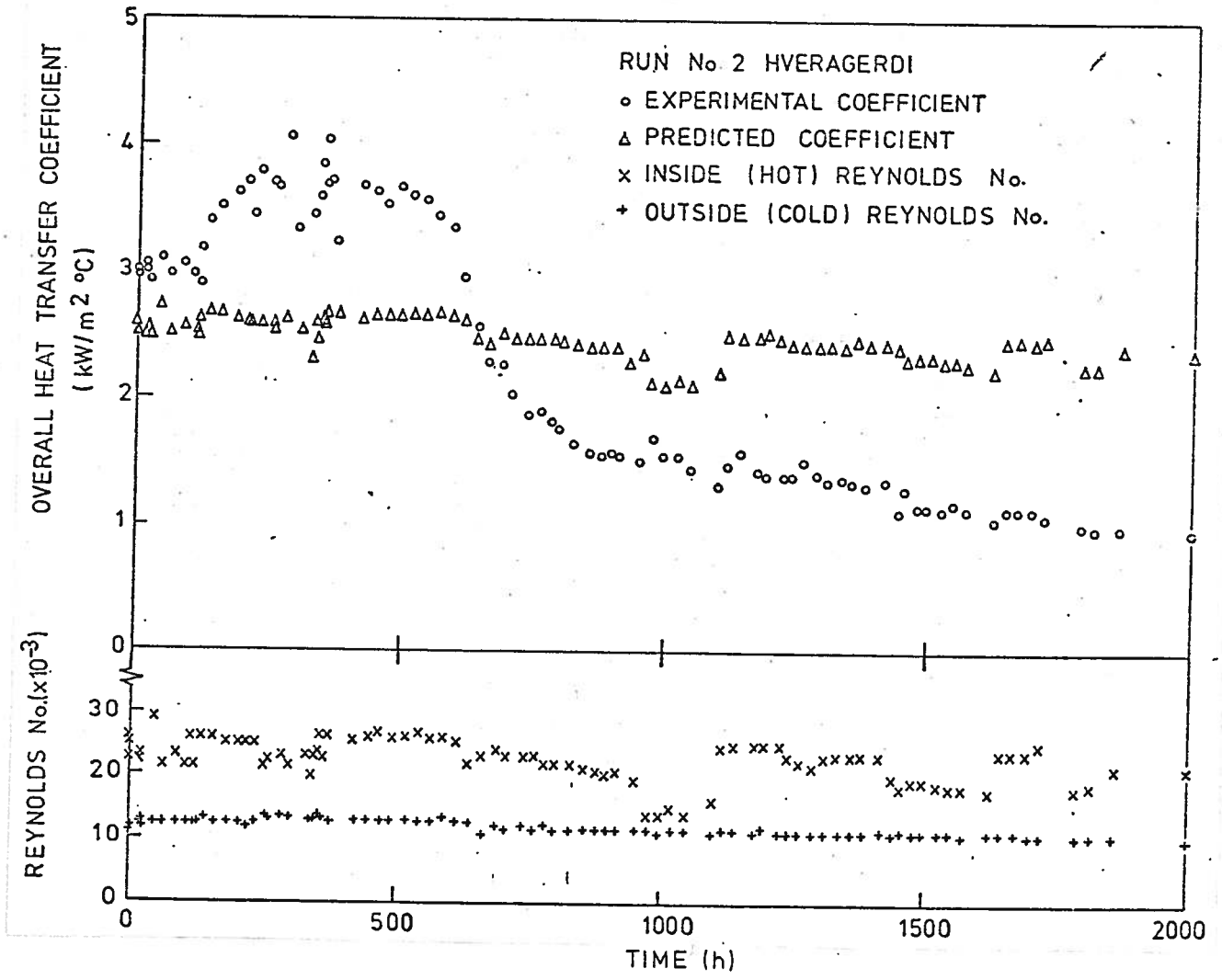

FIG. 6. OVERALL HEAT TRANSFER COEFFICIENT AND REYNOLDS NUMBER vs TIME AT HVERAGERDI - RUN 2.